Korean J. Chem. Eng., **26**(6), 1800-1805 (2009)
DOI: 10.2478/s11814-009-0269-5

Morphologies and properties of NiO particles prepared from $NiCl_2 \cdot 6H_2O$ by spray pyrolysis

Dong-Jun Kang and Sun-Geon Kim†

School of Chemical Engineering and Materials Science, Chung Ang University,
221, Huksuk-dong, Dongjak-gu, Seoul 156-756, Korea
(*Received 17 August 2007 • accepted 28 April 2009*)

Abstract−Nickel oxide particles were prepared by spray pyrolysis of aqueous solution of $NiCl_2 \cdot 6H_2O$. In the reactor the salt droplets were first converted to hollow particles by drying and then they were collapsed by oxidation to reduce their size. Each oxide particle was composed of many small nuclei with voids among them due to extremely low rate of sintering. The particle size decreased with the temperature as the sintering and crystallization proceeded. The size as well as the crystallinity of the particles increased with the initial salt concentration. When the salt droplets were preliminarily dried in diffusion dryer before entering the reactor, the collapse of the particles was considerably reduced, resulting in lower hollowness and higher sphericity. Numerical simulation on the drying of the droplets provided insight on the initial stage of spray pyrolysis.

Key words: NiO Particles, Spray Pyrolysis, $NiCl_2 \cdot 6H_2O$, Droplet Evaporation

INTRODUCTION

Spray pyrolysis has been successfully used to prepare spherical particles of metals, metal oxides and nonoxides [1], polymers [2], and composites [3], the last of which are difficult to prepare by other methods. However, it has not been easy yet to control the morphology of the particles produced by spray pyrolysis. This is because a variety of elementary processes are involved both consecutively and simultaneously within a single droplet during the overall spray pyrolysis [4]: they include, for producing metal oxide or metal particles, drying of the droplet, precipitation of precursor salt, decomposition of crystalline water if any, chemical transformation of the salt to oxide and/or to metal, and intraparticle sintering to form final structure of the product particles. Most of them were initiated from the surface of the droplet or the particle thereof by its interaction with surroundings. Different rates of these processes produce particles with a variety of morphologies [5] such as densely solid, hollow, porous, burst-out and even nano-sized particles.

Jayanthi et al. [6] proposed a criterion whether the particles formed by spray pyrolysis were hollow or not in numerical simulation on drying Zr(OH)Cl droplets. According to them, the primitive particles are formed when salt concentration at droplet surface becomes critically supersaturated. Their criterion was whether at the moment the concentration in the droplet center reached the saturation or not. Their approach was extended by Yu et al. [7] and Lenggoro et al. [8] with little modification. On the other hand, Jain et al. [9] emphasized the importance of salt(A)-to-product(B) transformation rather than salt precipitation, focusing the effect of density increase or volume contraction during the transformation. They proposed that hollow particle of B would form if the theoretical volume of B calculated from A in a droplet is below 0.16 times that of the primitive particles. The numerical value of 0.16 was given by the percolation theory [9]. Che et al. [4] proposed a qualitative model for particle morphologies but they advanced considering intraparticle sintering and phase separation as well as a variety of intraparticle reaction.

On the other hand, preparation of nickel particles by spray pyrolysis has been very attractive to produce spherical, solid and highly crystalline particles with diameters from 0.1 to 1.5 μm and smooth surfaces. In the course of their preparation nickel oxide particles were frequently observed as an intermediate, whose morphology varies with process variables quite differently from that of the final nickel particles. While Nagashima et al. [10] carried out spray pyrolysis of $Ni(NO_3)_2 \cdot 6H_2O$ aqueous solution with 20 vol% H_2 in N_2 they obtained nickel oxide particles at low H_2 flow rate between 500 and 700 °C, which were so fragile as to be easily broken into fragments. Stovic et al. [11] prepared, from $NiCl_2 \cdot 6H_2O$ with N_2 only between 700 and 900 °C, ideally spherical nickel oxide particles having the average diameter larger than the theoretically expected one. They discussed that the sphericity came from sufficient residence time in the reactor, while the size increase was caused by partial coalescence of droplets. Che et al. [12], however, prepared hollow nickel oxide particles with rough surface around 300 °C from spray pyrolysis of aqueous solution of $Ni(NO_3)_2 \cdot 6H_2O$ with 10 vol% H_2 in N_2. They also prepared nickel oxide particles from the same salt with N_2 only, which remained hollow all the way to 1,200 °C due to the high sintering temperature of the oxide.

In our study, nickel oxide particles were prepared by spray pyrolysis of aqueous solution of $NiCl_2 \cdot 6H_2O$. The nature and initial concentration of the salt and furnace set temperature were varied one by one to investigate their effects on the morphology, size, chemical composition and crystallinity of the particles produced. Preliminary drying was added to investigate its effect on the particle morphology, minimizing overlapping with other elementary processes. To understand the initial stage of droplet-to-particle conversion, we also did a numerical analysis on drying of aqueous nickel salt droplets.

†To whom correspondence should be addressed.
E-mail: sgkim@cau.ac.kr

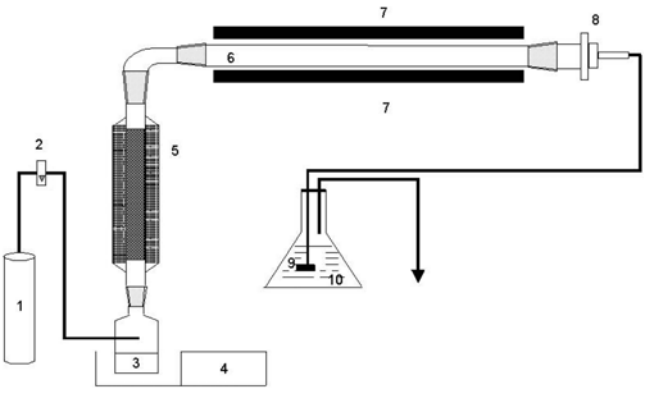

Fig. 1. Schematic diagram of overall experimental apparatus.

1. Ar gas
2. Flow meter
3. Nickel salt solution
4. Ultrasonic nebulizer
5. Diffusion dryer
6. Reactor
7. Electrical furnace
8. Filter
9. Bubbler
10. NaOH solution

EXPERIMENTAL

Fig. 1 shows the overall apparatus for the preparation of nickel oxide particles by spray pyrolysis, consisting of ultrasonic nebulizer, diffusion dryer, tubular reactor in electrical furnace, filter and acid gas absorber. Nickel salt solution with various concentrations (reference concentration was 0.5 M) maintained at 30 °C was nebulized indirectly at a rate of 15 ml/h . The droplets were carried by argon gas (99.99%) at 2,500 ml/min (reference value), via diffusion dryer if necessary, to electrically heated tubular reactor 800 mm long with the diameter of 32 mm. Axial distribution of the temperatures inside the reactor was measured with carrier gas flow as shown in Fig. 2 under the furnace set temperature of 950 °C (reference value). The furnace set temperature was obtained only in the middle 1/3rd of the furnace length. The diffusion dryer was introduced to study the effect of drying extracted from main spray pyrolysis. It was 800 mm-long concentric tubes composed of 36 mm ID inner tube made of steel mesh and 56 mm ID outer tube of Pyrex. Pellets of silica gel were packed in its annular space to dry the carrier gas flowing in the inner tube so that the water in the droplets could evaporate.

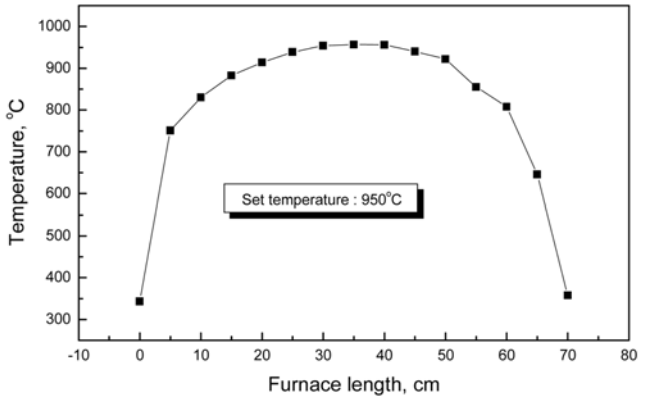

Fig. 2. Axial distribution of temperature in the reactor at furnace set temperature at 950 °C.

The droplets introduced to the reactor were thus two types, those passing through the diffusion dryer and those directly from the nebulizer. In addition to the mode of drying, the process variables included the initial concentration of the nickel salt and furnace set temperature in order to investigate their effect on the size, morphology, crystallinity and chemical nature of the product particles.

The particles exiting from the reactor were collected by filter. Both thermophoresis of particles and condensation of water vapor were minimized by shortening and heating space between the reactor exit and filter. The water vapor and acid formed was finally absorbed in caustic solution before exhausting the waste gas.

1. Characterization of Particles

Size and shape of the particles prepared were observed with a scanning electron microscope (SEM, Philips Co, Philips 515) and transmission electron microscope (TEM, Carl Zeiss-EM912 Omega). Number average diameters of the particles were obtained by measuring at least 100 particles shown in SEM images of each sample. Crystallinity of particles was obtained with X-ray diffractometer (XRD, Scintag-SDS 2000). Atomic bonds in the particles were analyzed with Fourier transformed infrared spectroscope (FT-IR, Perkin Elmer FT-IR 1615). Energy dispersive spectroscope (EDS, Model: Voyager, Noran) was used to analyze chemical composition of the particles. Thermogravimetric-differential thermal analyzer (TG-DTA, MAC Science, TG-DTA 200) was used to see thermal and chemical transformation of reagent $NiCl_2 \cdot 6H_2O$ under environment of argon at a rate of temperature rise of 20 °C/min.

NUMERICAL SIMULATION OF DROPLET DRYING AND SALT PRECIPITATION

Droplet drying and salt precipitation, the initial stage of droplet-to-particle conversion, was investigated by numerical simulation. Its detailed procedure was explained elsewhere [6-8]. System of the ordinary differential equations resulting from material and energy balances of a droplet, and Fick's second law of diffusion within the droplet was solved simultaneously by an ordinary differential equation solver, IVPAG in IMSL package. Since no information on the critical supersaturation concentration of $NiCl_2 \cdot 6H_2O$ in water was given, calculation was stopped when the solute concentration at center of the droplet just exceeded the equilibrium solubility. At the moment the ratio of the surface concentration to the equilibrium solubility was checked as to whether it was higher than the values of supersaturation ratio generally known, for example, 1.4 of Zr(OH)Cl [6,8]. We investigated the drying behavior of the salt droplet first at room temperature and then at temperatures simulating the actual temperature distribution in the reactor shown in Fig. 2. The former corresponded to the drying in diffusion dryer, while the latter to direct thermal drying. In addition, the effects of the initial molar salt concentration on the morphology and size of the particles were studied for the direct thermal drying only. The diameter of initial droplet was assumed 3 μm [10]; otherwise the same reference values were used as those in the experiments.

RESULTS AND DISCUSSION

1. Results of Numerical Simulation

Fig. 3 shows the droplet behaviors for diffusion drying and ther-

mal drying, respectively. As shown in Fig. 3(a), for thermal-dried droplets the surface salt concentration reached twice the center concentration at the moment the latter reached the equilibrium solubility. It was thus highly probable that the particles would be hollow. On the other hand, for diffusion-dried droplet, the ratio at the end of calculation as described above was only 1.1, too low for the primitive particles to form. Thus, the calculation continued until the surface concentration reached twice of the equilibrium solubility, whose result is shown in Fig. 3(a). The radial distribution of salt concentration in this droplet was still close to uniform, implying that the particles obtained would be not hollow but solid. Fig. 3(b) shows the time evolutions of droplet diameter. Diffusion-dried droplets take much more time to reach their final diameter than thermal-dried droplets, while the final diameters for the two cases are almost the same. Since the rate of size decrease was being substantially reduced at the end of calculation, it is supposed the size of the final droplets

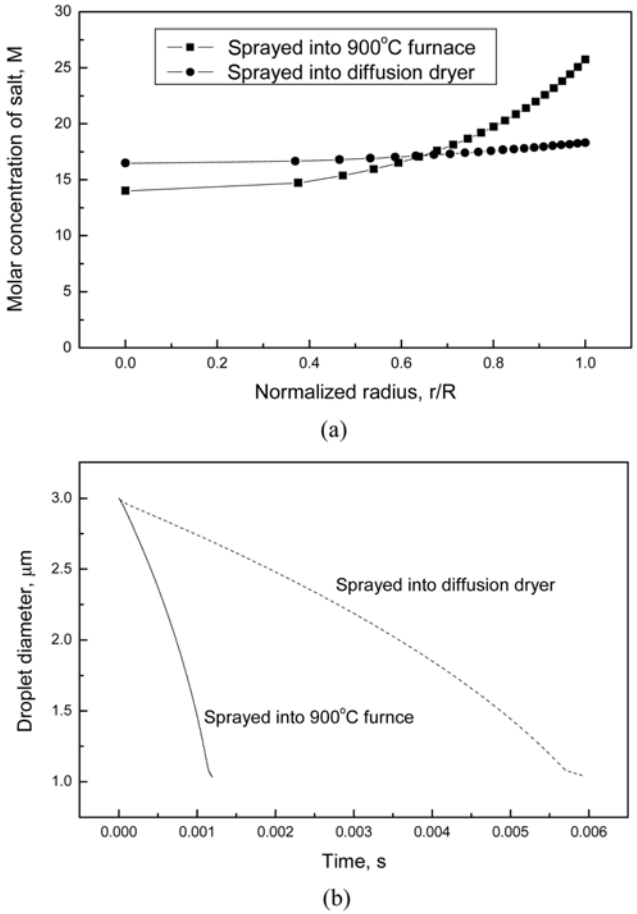

Fig. 3. Effect of drying modes of $NiCl_2 \cdot 6H_2O$ droplet on (a) radial distribution of molar concentration in droplet and (b) time evolution of droplet diameter under reference condition.

Table 1. Comparison of diameters of dried particles calculated from Eq. (1) and from numerical simulation

Initial salt concentration, M	0.1	0.5	2
Eq. (1), nm	566	967	1536
Numerical simulation, nm	604	1030	1640

obtained is not far from that of ultimately dried salt particles as well as the primitive particles. For the thermal-dried droplets, the initial salt concentration of the droplet did not affect the radial distribution of the concentration and thus the particle morphology but did the size of the primitive particles, as shown in Table 1.

Theoretical diameter of the solid particles d_p is related to the original droplet diameter d_d as follows:

$$d_p = d_d\left(\frac{Mw \cdot C_M}{1000 \cdot \rho_p}\right)^{1/3} \quad (1)$$

where Mw and ρ_p is the molecular weight and density of the material consisting of the particles, respectively, and C_M molar concentration of the salt. The variation of the primitive particle size from numerical simulation is compared with that of the theoretical particle size computed from the Eq. (1) with respect to the initial salt concentration, as shown in Table 1. The Table indicates that the former particles are larger than the latter in diameter by 5 to 7%, and this contributes to the particle volume as much as 25%. This void supposedly resulted in nonhollow but less dense or homogeneously porous structure for the diffusion dried particles and centrally hollow but dense crust-like structure for the directly thermal dried particles. Thus, while the diffusion-dried particles experience further drying and salt-to-oxide conversion in the reactor, their size would be hardly contracted due to their original solidness, in spite of substantial volume contraction during the oxidation. On the other hand, by subsequent oxidation the thermal-dried particles would be contracted by filling the hollowness to retreat their surface even though sintering of oxide was hardly expected.

2. Particles Obtained by Diffusion Drying

Droplets being dried through diffusion dryer, when filtered at its outlet, are shown in Fig. 4. The particles shown in the figure seem relatively soft and moist with very smooth surface, as expected, while neither hollow nor burst-out particles are observed. From the XRD patterns the particles were not $NiCl_2 \cdot 6H_2O$ but $NiCl_2 \cdot xH_2O$ where $0<x<6$, and thus some crystalline water seemed already to escape.

3. Effect of Drying Stages

Fig. 5 shows SEM pictures of the particles prepared by spray pyrolysis of aqueous solution of $NiCl_2 \cdot 6H_2O$ with and without diffu-

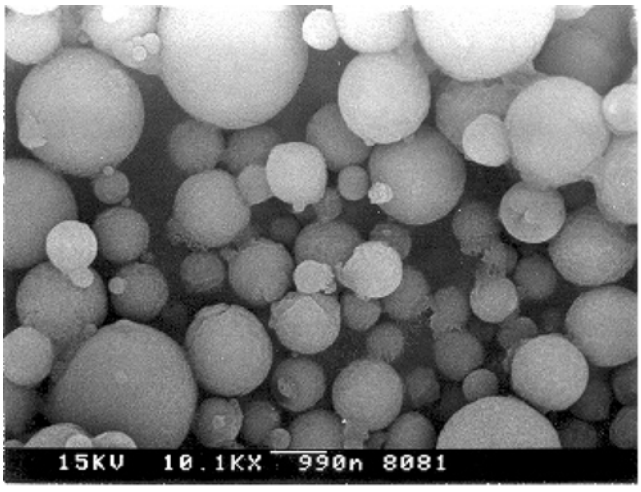

Fig. 4. SEM pictures of $NiCl_2 \cdot 6H_2O$ droplets passing through diffusion dryer under reference condition.

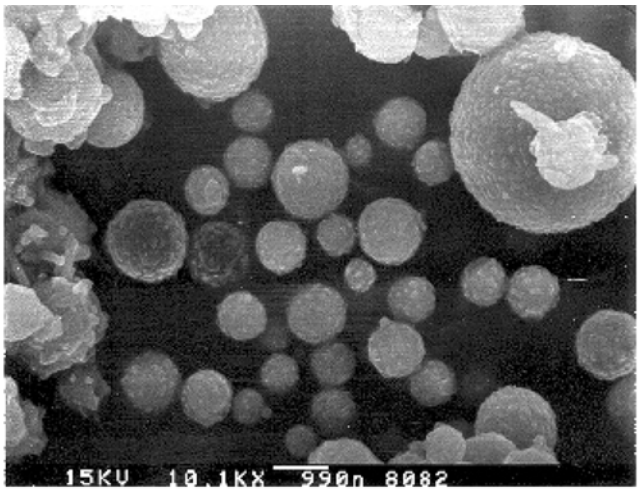

(a)

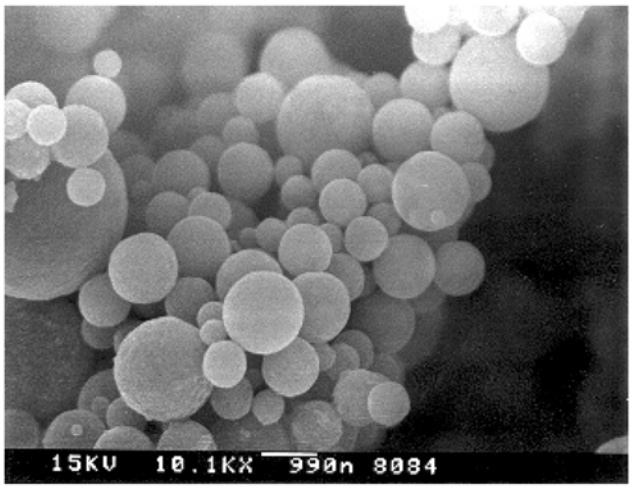

(b)

Fig. 5. SEM pictures of particles prepared from $NiCl_2 \cdot 6H_2O$ solution with (a) thermal drying only and (b) diffusion+thermal drying at reference condition.

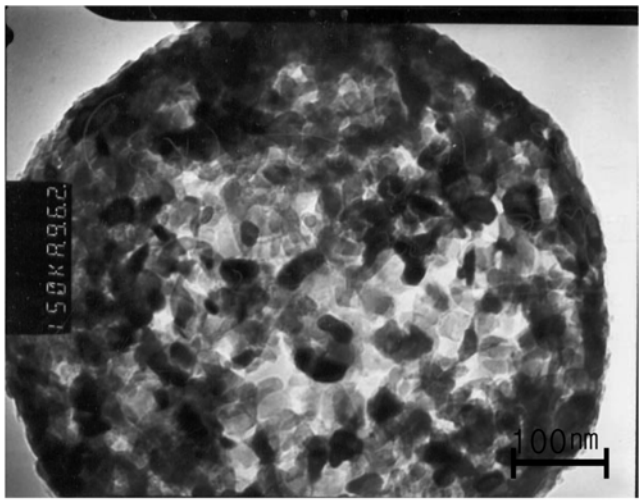

(a)

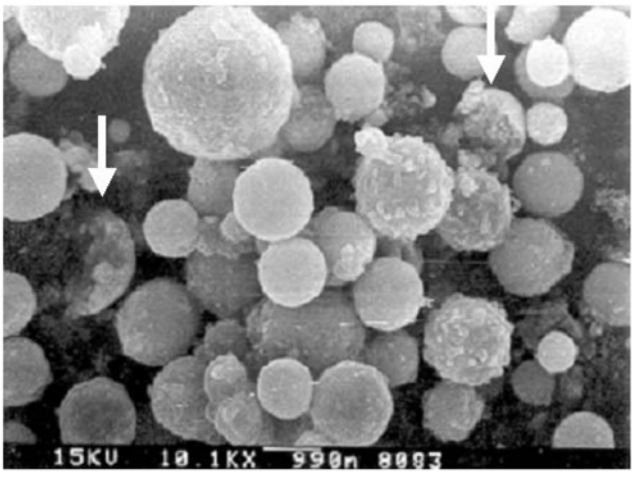

(b)

Fig. 6. (a) TEM and (b) SEM pictures of particles prepared from $NiCl_2 \cdot 6H_2O$ droplets with thermal drying only, otherwise under reference condition. Arrows in SEM image indicate broken particles showing solidness of particles made of hardly sintered nuclei.

sion drying. As described before, the oxide particles via diffusion dryer were more spherical with smoother surfaces succeeding to the droplet just solidifying, the primitive salt particles in shape and size. The particles experiencing direct pyrolysis, on the other hand, have rougher surface and are sometimes farther from sphericity losing their droplet nature. Fig. 6(a) shows TEM picture of the particles prepared by direct pyrolysis. It is noted in the figure the single oxide particle consisted of very small primary particles, the nuclei generated during salt-to-oxide conversion. The broken particles indicated by arrows in the SEM image in Fig. 6(b) evidence the solidness of the particles made of the oxide nuclei, which are hardly sintered. The existence of the primary particles or nuclei without sintering supports the difficult sintering nature of the oxide as described by Che et al. [11].

4. Effect of Temperature

Nickel oxide was identified from the XRD patterns of the particles prepared at 500 °C and up, irrespective of drying modes. Fig. 7 shows the XRD patterns of the particles prepared by direct pyrolysis at different furnace set temperatures. It is noted that heights and half widths of the peaks increase with the temperature, which implies that the sizes of crystallites also increase with it. The growth of the crystallites was seemingly related to the neck formation between the nuclei as well as the increased conversion to nickel oxide. The neck formation is the early stage of sintering, some evidence of which is observed in Fig. 6(a). However, the peaks of the chloride appear up to 1,000 °C, even though they decrease with the temperature, which implies the oxidation is not complete.

The directly pyrolyzed particles obtained at higher temperature were smaller and less spherical with rougher surface, which again shows the effect of the collapse. Due to the higher conversion to nickel oxide at higher temperature as shown in Fig. 7, more volume reduction would result in more collapse. Fig. 8 shows the effect of furnace set temperature on number average diameter of the oxide particles prepared via two modes of drying. The average size of the particles significantly decreases up to 800 °C, which is proba-

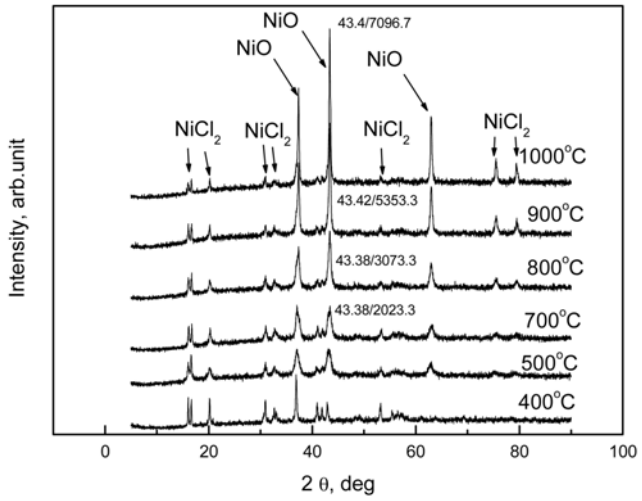

Fig. 7. XRD patterns of particles prepared from $NiCl_2 \cdot 6H_2O$ droplets with thermal drying only at different furnace set temperatures, otherwise under reference condition.

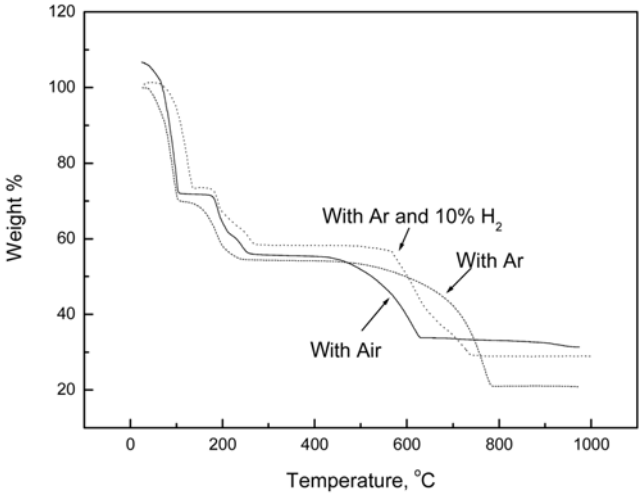

Fig. 9. Thermogravimetric analysis of reagent-grade $NiCl_2 \cdot 6H_2O$ with heating rate of 20 °C/min under air, Ar and 10 vol% H_2 in Ar atmospheres.

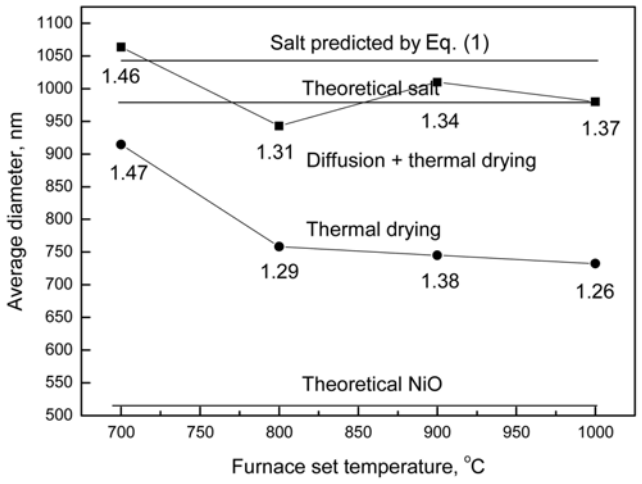

Fig. 8. Effect of furnace set temperature on diameter of particles prepared from $NiCl_2 \cdot 6H_2O$ droplets, otherwise under reference condition (Geometric standard deviations are shown in numbers).

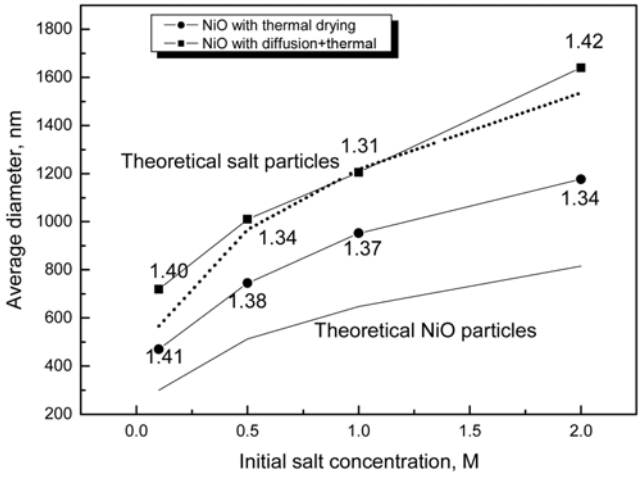

Fig. 10. Effect of initial salt concentration on diameter of particles prepared from $NiCl_2 \cdot 6H_2O$ droplets, otherwise under reference condition (Geometric standard deviations are shown in numbers).

bly related to the oxidation, as will be discussed later. This highly implies the volume reduction would end up with the oxidation rather than sintering. Since all the primitive particles are supposed to start with the similar sizes, despite different morphology depending on the drying modes, as discussed before, the particles from direct pyrolysis have smaller size than those experiencing preliminary drying whose size is not far from that of theoretical salt particles regardless of the temperature. This, therefore, supports that the former particles would experience considerable volume reduction by filling the central hollowness while the latter would do a little, if any, due to their relative solidness as described before.

Fig. 9 shows the result of thermogravimetric analysis of reagent $NiCl_2 \cdot 6H_2O$ in argon, air and 10% H_2 in argon with the rate of temperature rise, 20°/min. Regardless of gas environments, the first weight loss occurs due to the partial decomposition of four moles of crystalline water per mole of the salt below 100 °C and then the rest two moles of water escape between 160 and 220 °C. The sample in the air environment is oxidized between 400 °C and 600 °C. The overall weight loss from the initial salt to nickel oxide is close to 68.6% expected. It is not clear how the oxidation takes place in the actual spray pyrolysis since the water vapor exists in place of the air. However, the situation would not be quite different in the actual reactor except that the oxidation started at 500 °C and still remained incomplete even at 1,000 °C, as discussed before, due to the short residence time in the reactor. In the same figure, it is believed that the reduction to nickel rather than the oxidation would occur even in argon environment but at higher temperature than in the argon-hydrogen environment since all the water vapor escapes up to 220 °C from the sample.

5. Effect of Initial Salt Concentration

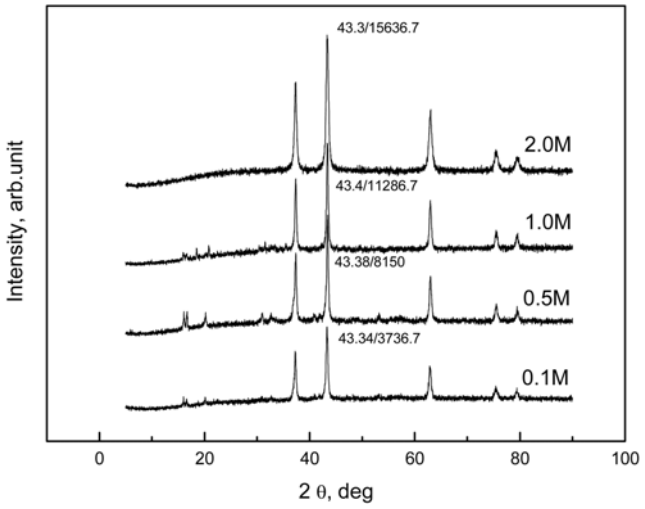

Fig. 11. XRD patterns of particles prepared from $NiCl_2 \cdot 6H_2O$ solution with thermal drying only at different initial salt concentration, otherwise under reference condition.

Increase in the initial salt concentration clearly made the size of the particles increase. Other significant changes such as hollowness and surface smoothness were not observed, as expected in the numerical simulation. Fig. 10 shows the average diameter of the particles prepared with respect to the initial salt concentration. The theoretical diameters of both the salt and oxide particles calculated by Eq. (1) are also shown in the figure. The size of the particles, irrespective of drying modes, increases with the concentration. The findings as described before were confirmed: The particles prepared via the diffusion dryer have diameters close to those of the theoretical salt particles and larger than those of the particles by direct pyrolysis, while all the oxide particles are larger than theoretical oxide particles. As shown in the figure, it is noted that the sizes of the directly pyrolyzed particles locate apparently in the same relative positions between the sizes of theoretical salt and nickel oxide particles. This means the particles prepared have the same morphology such as the size and the packing density of the oxide nuclei at the given temperature irrespective of the initial salt concentrations.

Fig. 11 shows the XRD patterns of the particles prepared by direct pyrolysis at different initial salt concentrations. As shown, the height of nickel oxide peaks considerably increases with the concentration, compared to any other variable such as the furnace set temperature. However, the half width of the peaks did not vary with the concentration, which implies that the size of crystallites is independent of the concentration at a given temperature. Thus the increase in the crystallinity of the particles with the concentration supposedly comes from the increase in the sources of crystallites.

CONCLUSIONS

Nickel oxide particles were prepared by spray pyrolysis of aqueous solution of $NiCl_2 \cdot 6H_2O$. In the early stage of the spray pyrolysis the salt droplets were dried at the surface to form hollow particles and subsequently collapsed by oxidation to lose their sphericity. The oxide particles were made of many isolated nuclei before sintering. The sintering as well as crystallization proceeded with the increase of the reactor temperature. The crystallinity as well as particle size increased with the initial salt concentration under the given reactor condition. When the diffusion dryer was placed before the reactor, the morphology of the oxide particles was considerably improved in the sphericity, surface smoothness and solidness. Droplet-to-salt conversion was simulated by numerical analysis of droplet drying to elucidate the initial stage of spray pyrolysis, which could not be observed by experiment.

ACKNOWLEDGMENT

This Research was supported by the Chung-Ang University Research Grant in 2009.

REFERENCES

1. Y. Arai, *Chemistry of powder production*, Chapman & Hall, London (1996).
2. D. S. Shin, E. K. Oh and S. G. Kim, *Aerosol Sci. & Technol.*, **24**, 243 (1996).
3. C. B. Martin, R. P. Kurovsky, G. D. Maupin, C. Han, H. J. Javadpour and I. A. Aksay, *Ceramic powder science III, ceramic transactions*, ed. by G. L. Messing , S.-I. Hirano and H. Hausner, The Amer. Ceram. Soc. Inc., Westerville, Ohio, 12 (1990).
4. S. C. Che, O. Sakurai, K. Shinozaki and N. Mizutani, *J. Aerosol. Sci.*, **29**, 271 (1998).
5. K. Okuyama, K. Ohshima and K. Tsudo, *Kona*, **9**, 79 (1991).
6. G. V. Jayanthi, S. C. Zhang and G. L. Messing, *Aerosol. Sci. & Technol.*, **19**, 478 (1993).
7. H. F. Yu and W.-H. Liao, *Int. J. Heat Mass Transfer.*, **41**, 993 (1998).
8. I. W. Lenggoro, T. Hata, F. Iskandar, M. M. Lunden and K. Okuyama, *J. Mater. Res.*, **15**, 733 (2000).
9. S. Jain, D. J. Skamser and T. Y. Kodas, *Aerosol. Sci. & Technol.*, **27**, 575(1997).
10. K. Nagashima, M. Wada and A. Kato, *J. Mater. Res.*, **5**, 2828 (1990).
11. S. Stovic, I. Ilic and D. Uskokovic, *Mater. Lett.*, **24**, 369 (1995).
12. S. L. Che, K. Takada, K. Takashima, O. Sakurai, K. Shinozaki and N. Mizutani, *J. Mater. Sci.*, **34**, 1313 (1999).